Quantum Electronics **35** (11) 1075 – 1078 (2005)

LASER APPLICATIONS IN MEDICINE

PACS numbers: 42.62.Be; 42.25.Fx; 42.65.Re
DOI: 10.1070/QE2005v035n11ABEH012794

Effect of glucose concentration in a model light-scattering suspension on propagation of ultrashort laser pulses

A.P. Popov, A.V. Priezzhev, R. Myllylä

***Abstract*. The propagation of laser pulses in the 2 % aqueous solution of intralipid – a suspension of lipid particles with optical properties close to those of the human skin, is numerically simulated at different glucose concentrations. The temporal profiles of 820-nm laser pulses diffusely backscattered from a flat, 2-mm thick solution layer are simulated. The laser pulse profiles are detected by fibreoptic detectors of diameter 0.3 mm with the numerical apertures 0.19, 0.29, and 0.39. It is shown that this method can be used to detect changes in the glucose level in the physiological concentration range (100 – 500 mg dL^{-1}) by monitoring variations in the peak intensity and area of the laser pulse temporal profile (pulse energy).**

Keywords: *propagation of light, laser pulses, time-of-flight spectroscopy, numerical simulation, skin model, optical diagnostics, Monte-Carlo method, intralipid.*

1. Introduction

At present the problem of diabetes is one of the acute social problem determining the quality of human life. Over 140 million people suffer from diabetes worldwide. As predicted in [1], this number will increase up to 300 million in 2025. The disease develops either due to deficiency of the hormone insulin produced in the human organism by the pancreas or due to inability of cells to assimilate this hormone. During this disease, the glucose level in blood increases, which can cause coma or even death of a patient. Therefore, the measuring of the glucose level in blood is an urgent problem. This level correlates within 20 % with the glucose level in the intercellular fluid with the time delay of about 30 min [2]. At present, patients often perform monitoring of the glucose level themselves by analysing a drop of blood taken by finger puncturing. This procedure should be performed several times per day, which is very inconvenient for patients. The development of new non-invasive, in particular, optical methods for measuring the glucose content in human tissues and their introduction to medicine would be the efficient solution of this problem.

By now several such methods have been proposed. They include the methods based on absorption and scattering of light in the near-IR spectral range [3 – 6], polarimetry [7, 8], Raman spectroscopy [9], photoacoustics [10, 11], time-of-flight spectroscopy [12], optical coherence tomography [13], etc. However, the common disadvantage of all these methods is their low sensitivity in the physiological range of the glucose level (100 – 500 mg dL^{-1}). In particular, by detecting a signal in the forward direction with the use of 30-ps pulses, the authors of paper [14] have managed to measure only very high glucose concentration (4 % – 8 % wt, i.e., 4000 – 8000 mg dL^{-1}) in a 1-cm cell with the 2 % intralipid solution.

Femtosecond lasers emitting in the near-IR range are promising tools for such investigations. Their advantages over cw lasers are a greater penetration depth into tissues, a small coherence length [which is important for the high-resolution tomography (15)], and a low concentration of the detected energy in a narrow time interval, which rises the detection sensitivity. Near-IR femtosecond lasers can be also used for measuring the glucose level in human skin.

In this paper, by using Monte-Carlo simulations, we show that the time-of-flight spectroscopy with the use of femtosecond pulses in the scheme of detecting backward scattered signals is a promising method for measuring the glucose level.

2. Materials and methods

We simulated the propagation of laser pulses inside a 2-mm flat layer of the intralipid solution modelling the optical properties of the human skin in the near-IR region [16]. Intralipid is a fatty emulsion which is used for intravenous nutrition. According to the manufacturer [17, 18], 500 mL of the 10 % intralipid contain 11.25 g of glycerol, 6 g of lecithin, 50 g of soy oil, and 430.5 g of water. The size of particles in the emulsion changes in a broad range from 25 to 675 nm (the average size is 97 nm) [19], and the shape of smaller particles differs stronger from a sphere than that of larger particles.

Figure 1 shows the scheme of the experimental setup. We used a Ti : sapphire laser emitting 100-μJ, 820-nm, 50-fs pulses with a pulse repetition rate of 50 Hz. The optical

A.P. Popov Department of Physics, M.V. Lomonosov Moscow State University, Vorob'evy gory, 119992 Moscow, Russia;
A.V. Priezzhev Department of Physics, International Laser Center, M.V. Lomonosov Moscow State University, Vorob'evy gory, 119992 Moscow, Russia; e-mail: dwelle@rambler.ru, avp2@mail.ru;
R. Myllylä Optoelectronics and Measurement Techniques Laboratory, Faculty of Technology, University of Oulu and Infotech Oulu, P.O. Box 4500, Oulu, 90014 Finland; e-mail: risto.myllula@ee.oulu.fi

Received 5 July 2005; revision received 19 August 2005
Kvantovaya Elektronika **35** (11) 1075 – 1078 (2005)
Translated by M.N. Sapozhnikov

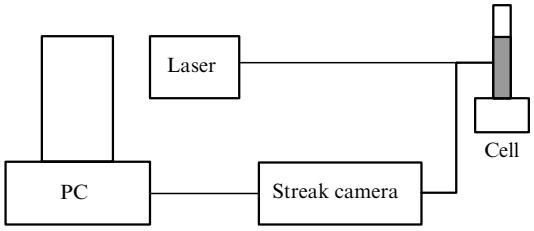

Figure 1. Scheme of the setup used in simulations.

properties of the intralipid solution were calculated assuming the scattering anisotropy factor $g = 0.6244$, the scattering coefficient $\mu_s = 5.16\ \text{mm}^{-1}$, the absorption coefficient $\mu_a = 0.002\ \text{mm}^{-1}$ (the same as for water, because intralipid does not absorb in the near-IR region), and the refractive index $n_{int} = 1.325$ (water) taken from [19]. The outer side of the intralipid layer is in contact with air ($n = 1$). Femtosecond laser pulses are simulated by pulses of zero duration (temporal delta function), which is acceptable in the geometry used, because the FWHM of detected pulses is $\sim$3 ps. The pulses are injected into the solution on the outer side of the layer at the point with coordinates (0, 0, 0). Pulses scattered diffusely backward are detected with a flat circular detector of diameter 0.3 mm (coaxial with the laser beam) modelling optical fibres with the numerical apertures NA = 0.19, 0.29, and 0.39, which correspond to the detection angles in the medium equal to 8.24°, 12.64°, and 17.12°. The spectral width of pulses was neglected because the optical properties of the intralipid solution (and skin) change insignificantly in the near-IR range. Such a detection scheme corresponds to *in vivo* measurements on skin. Detection was performed with a time resolution of 0.1 ps.

After the glucose adding into intralipid, the difference between the refractive indices of light-scattering fatty particles of intralipid and surrounding liquid (water) decreases, resulting in a change in the propagation of light in the medium. The influence of glucose on the optical parameters of a light-scattering medium is described by the expressions [13, 20, 21]

$$n = 1.325 + 1.515 \times 10^{-6} C, \tag{1}$$

$$\mu_s = (1 - 0.0022C/18)\mu_{sm}, \tag{2}$$

$$g = (1 + 0.000007C/18)g_m, \tag{3}$$

where C is the glucose concentration (mg dL^{-1}); g_m and μ_{sm} are the scattering anisotropy factor and scattering coefficient of the intralipid solution, respectively, before the glucose adding. One can see from these expressions that the scattering coefficient experiences the greatest relative change – 22 % per mmole L^{-1} (which corresponds to 18 mg dL^{-1}).

The propagation of radiation inside a layer was simulated by the Monte-Carlo method [22] representing the algorithm for calculating the transport of photons in a three-dimensional medium by means of random tests. The calculations were performed by using the software code developed in the Delphi® software environment tested in many cases considered earlier by other authors. This algorithm is briefly described below.

The mean free path of a photon

$$L = -\frac{\ln(1 - \text{Random})}{\mu_s + \mu_a} \tag{4}$$

was determined at each step with the help of a built-in random number generator, where Random is a random value in the range 0 – 1; and scattering or absorption of a photon by an intralipid particle is determined by the ratio of μ_a and μ_s. After absorption or detection of a photon, the next photon is launched. The scattering angles φ and θ are calculated by the expressions [23]

$$\varphi = 2\pi\text{Random}, \tag{5}$$

$$\theta = \cos^{-1}\left\{\frac{1 + g^2 = [(1 - g^2)/(1 + g - 2g\text{Random})]^2}{2g}\right\}. \tag{6}$$

The angle θ is determined by the Henyey–Greenstein phase scattering function [24]

$$p(\theta) = \frac{1}{4\pi}\frac{1 - g^2}{(1 + g^2 - 2g\cos\theta)^{3/2}}. \tag{7}$$

The procedure continues until all photons are 'spent'. Each of the simulated pulses consists of 500 million photons, which provides a reasonable compromise between the statistical error and calculation time (about 5 h with P-IV 3 GHz, 1.5 GB). The algorithm is described in detail in our paper [25].

The preliminary calculations and comparison of the results obtained for intralipid layers of thickness 2 mm and 2000 mm showed that the pulse profiles detected in these two cases differed insignificantly, so that the use of the 2-mm thick layer is justified (although the skin and underlying tissues better correspond to a semi-infinite medium) and considerably reduces the calculation time (5 h vs 30 h with P-IV 3 GHz, 1.5 GB). This can be explained in terms of the transport mean free path l^*. This parameter for a strongly scattering medium shows at which distance the radiation at this wavelength becomes stochastic, i.e., photons 'forget' their initial propagation direction, and is determined by the expression

$$l^* = \frac{1}{\mu_s(1 - g) + \mu_a}. \tag{8}$$

For the simulated medium, $l^* = 0.5$ mm for $C = 0$ and 0.59 mm for $C = 1000$ mg dL^{-1}, and therefore the distant boundary of the layer does not play any substantial role.

3. Results and discussion

We considered in simulations the influence of glucose added at concentrations 0, 100, 300, 500, and 1000 mg dL^{-1} to the 2 % intralipid solution on the profiles of detected pulses. The value $C = 100$ mg dL^{-1} corresponds to the normal concentration of glucose in the human skin (blood) (70–160 mg dL^{-1}) [13], whereas the higher concentrations correspond to the excess level of glucose in tissues. The concentration 500 mg dL^{-1} causes coma (concentrations $C = 0$ and 1000 mg dL^{-1} were taken to observe the effect more distinctly). Typical time responses of the medium for

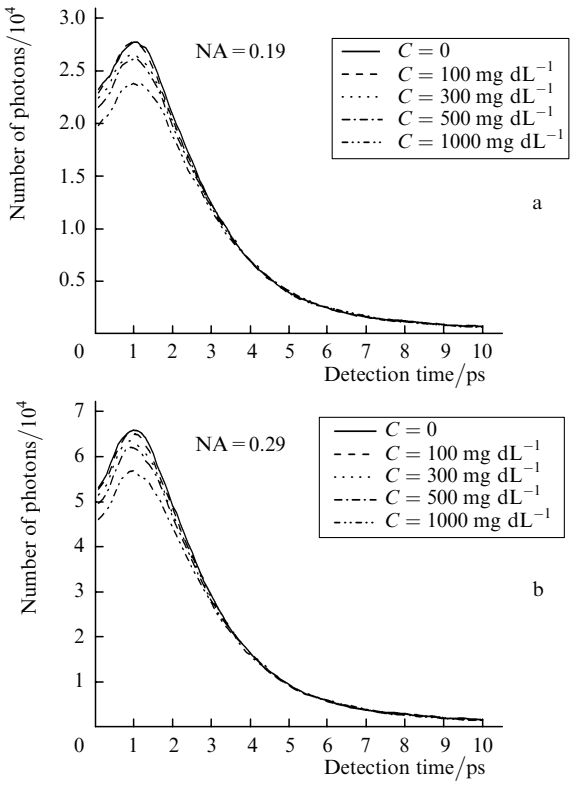

Figure 2. Temporal profiles of diffusely reflected delta pulses detected with fibre detectors with numerical apertures NA = 0.19 (a) and 0.29 (b) at different glucose contents in the solution. The curves are smoothed by the method of adjacent averaging over five points. Pulses are injected at the initial time $t = 0$.

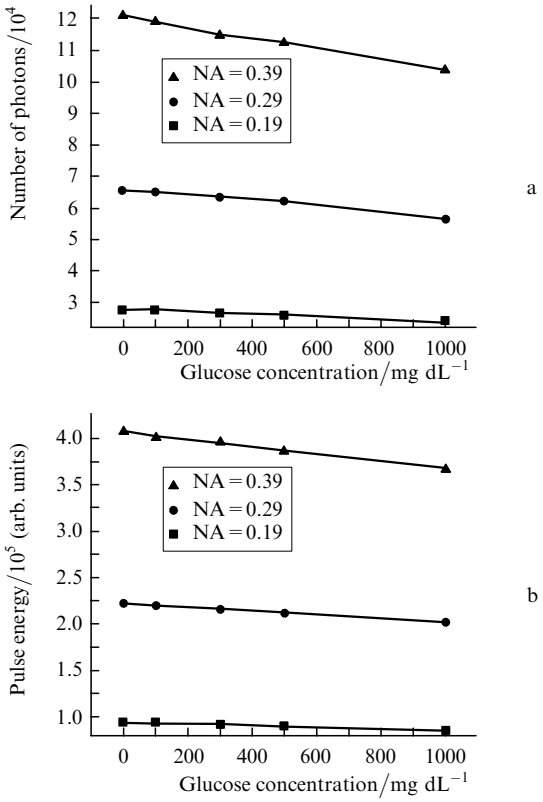

Figure 3. Dependences of the peak intensity (a) and area (b) of a backscattered pulse on the glucose concentration for different numerical apertures of a fibre sensor.

detectors with numerical apertures 0.19 and 0.29 are presented in Fig. 2. As the glucose content increases, the value of μ_s decreases and the factor g increases, resulting in a decrease in the number of photons detected in the backward direction. The curves in Fig. 2 are smoothed by the method of adjacent averaging over five points (corresponding to the time interval 0.5 ps). One can see that the difference between the curves is largest during the first three picoseconds of detection.

Figure 3 represents the dependences of the peak intensity and area under the curve (pulse energy) on the glucose concentration. The number of detected photons increases with increasing the numerical aperture of a detecting fibre. In practice, it is preferable to detect a higher intensity because in this case the useful signal is more distinctly observed against the noise background. A higher sensitivity of the glucose concentration measurement (a steeper slope of the concentration dependence) is observed for a larger numerical aperture. The absolute sensitivity of the glucose detection calculated from the dependence of the slope of the straight lines in Fig. 3 on the numerical aperture of the fibre is shown in Fig. 4. The values of slopes are negative because the signal decreases with increasing the glucose concentration. One can see that the pulse area (energy) depends on the numerical aperture (in absolute units) stronger than the pulse peak intensity. Note that, as the numerical aperture is doubled (from 0.19 to 0.39), the slope magnitude increases more than by a factor of four, both for the area and peak intensity.

Figure 5 shows the effect of the glucose concentration on the distribution of scattered radiation intensity over the

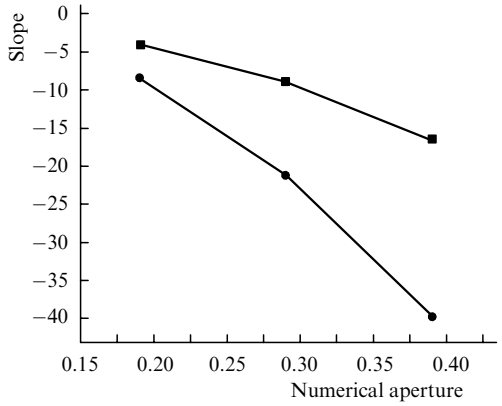

Figure 4. Absolute sensitivity of the glucose level detection by the peak intensity (■) and area (●) of a pulse at different numerical apertures of a fibre sensor.

layer depth. Laser pulses enter into the layer at the zero depth. As the scattering coefficient μ_s decreases, photons experience a smaller number of scattering events, and the medium becomes more transparent, cleared [26]. The intensity distribution maxima caused by diffuse scattering are located at some depth under the layer. A more detailed analysis shows that these maxima shift deeper as the glucose concentration is increased.

4. Conclusions

We have studied the possibility of monitoring the glucose content within the physiological range in a 2-mm thick

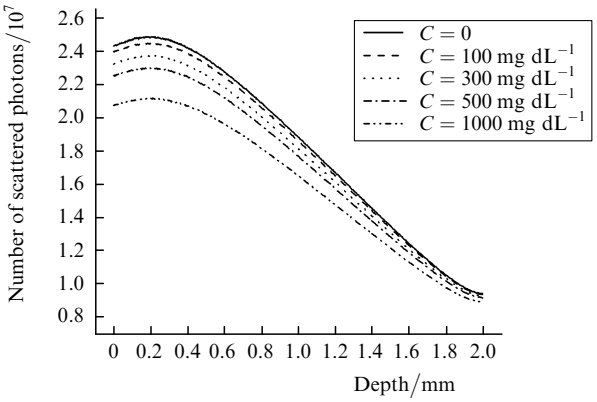

Figure 5. Intensity profiles of a scattered light pulse over the layer depth at different glucose concentrations.

layer of the 2 % intralipid solution simulating the optical parameters of the human skin by using femtosecond laser pulses approximated by the delta function in the near-IR region (820 nm). It is shown that the glucose level can be monitored by the peak intensity and energy of diffusely backscattered pulses detected with fibre detectors located on the outer surface of the layer. The pulse energy (area under the temporal pulse profile), which linearly depends on the glucose concentration, is most sensitive to variations in the glucose content. Detectors with large numerical apertures are preferable.

Acknowledgements. This work was partially supported by the Program 'Leading Scientific Schools of Russia' (Grant No. 2071.2003.4). A.P.P also thanks Infotech Oulu for support of this study.

References

1. Economic Consequences of Diabetes Mellitus in the US. *Diabetes Care*, **21**, 296 (1998).
2. Kost J. et al. *Nat. Med.*, **6**, 347 (2000).
3. Pan S. et al. *Anal. Chem.*, **68**, 1124 (1996).
4. Gabriely I. et al. *Diabetes Care*, **22**, 2026 (1999).
5. Robinson M. et al. *Clin. Chem.*, **38**, 1618 (1992).
6. Maier J. et al. *Opt. Lett.*, **19**, 2062 (1994).
7. Rabinovitch B. et al. *Diabetes Care*, **5**, 254 (1982).
8. Cote G. et al. *IEEE Trans. Biomed. Eng.*, **39**, 752 (1992).
9. Goetz M. et al. *IEEE Trans. Biomed. Eng.*, **42**, 728 (1995).
10. MacKenzie H. et al. *Clin. Chem.*, **45**, 1587 (1999).
11. Kinnunen M., Myllyla R. *J. Phys. D: Appl. Phys*, **38**, 2654 (2005).
12. Alarousu E. et al. *Proc. SPIE Int. Soc. Opt. Eng.*, **5474**, 33 (2004).
13. Larin K. et al. *Phys. Med. Biol.*, **48**, 1371 (2003).
14. Kinnunen M. et al. *Proc. SPIE Int. Soc. Opt. Eng.*, **5474**, 181 (2004).
15. Riemann I. et al. *Proc. SPIE Int. Soc. Opt. Eng.*, **5463**, 21 (2004).
16. Troy T., Thennadil S. *J. Biomed. Opt.*, **6**, 167 (2001).
17. Weast R. (Ed.) *Handbook of Chemistry and Physics* (Boca Raton, Fla.: CRC, 1978).
18. *The Merck Index* (Rahway, N.J.: Merck, 1976).
19. Van Staveren H. et al. *Appl. Opt.*, **30**, 4507 (1991).
20. Kohl M. et al. *Phys. Med. Biol.*, **40**, 1267 (1995).
21. Tarumi M. et al. *Phys. Med. Biol.*, **48**, 2373 (2003).
22. Sobol' I.M. *Chislennye metody Monte-Carlo* (Numerical Monte-Carlo Methods) (Moscow: Nauka, 1973).
23. Guo Z. et al. *J. Thermophys. Heat Transfer*, **14**, 504 (2000).
24. Henyey L.G., Greenstein J.L. *Astrophys. J.*, **93**, 70 (1941).
25. Popov A.P., Priezzhev A.V. *Proc. SPIE Int. Soc. Opt. Eng.*, **5068**, 99 (2003).
26. Zimnyakov D.A., Tuchin V.V. *Kvantovaya Elektron.*, **32**, 849 (2002) [*Quantum Electron.*, **32**, 849 (2002)].